



iJRASET

International Journal For Research in
Applied Science and Engineering Technology



INTERNATIONAL JOURNAL FOR RESEARCH

IN APPLIED SCIENCE & ENGINEERING TECHNOLOGY

Volume: 9 Issue: VI Month of publication: June 2021

DOI: <https://doi.org/10.22214/ijraset.2021.35014>

www.ijraset.com

Call:  08813907089

E-mail ID: ijraset@gmail.com

Fabrication and Analysis of Artificial Human Hand using 3D Printing Technology

R. Selvaraj¹, Dr. S. Sukumar², Mr. M. Saravanan³, Mr. G. Brithivi Raj⁴, Mr. P. Vijayakumar⁵

¹M.Tech Student, ^{2,3,4,5}Assistant Professor, Department of Mechanical Engineering, PRIST Deemed to be University, Thanjavur-613403

Abstract: Fabrication of human bone by 3d printing is playing an important role in medical applications. The various parts of human hand are made by PLA material by 3D printing Technology. The sequences of operations such as scanning, 3 Modeling, STL file and printing are involved for fabrication of Artificial human hand. In this work, we design, fabricate and analysis of artificial human bone by PLA material. The mechanical of Tensile strength, compressive strength, shear strength, bending strength and torque are analyzed by ANSYS software and hardness test measured with use of durometer and test values are analyzed by D scale. The chemical test are also conducted and compared with human bone values.

Keywords: Human hand, Modeling, 3D Printing, Testing, Comparison

I. INTRODUCTION

A. 3D Printing

With the emerging field of 3D printing, inexpensive 3D printed prosthetics are continually being developed to replace commercially developed prosthetics. High end prosthetics can cost thousands of dollars, which is unfortunately not affordable for many of those in need of prosthetic hands. As children grow, they need new prosthetics to fit their growing arms, which would cost more than a fully grown arm. One of the main advantages of 3D printed prosthetic hands is that they allow for custom prosthetics at a fraction of the price. While low income families may not be able to afford a new traditional prosthetic.

There are many benefits to 3D printed prosthetics such as cost, versatility, speed, growth, and comfort. A commercially made prosthetic can take up to months to both produce and calibrate and a 3D printed prosthetic takes about one day to print. 3D printed prosthetics are very versatile and customizable. The prosthetics can be designed to fit the specific user as well as various activities. In terms of growth, children who are in need of a prosthetic constantly grow out of their prosthetic until they have finished developing.

B. Rapid Prototyping

Rapid Prototyping (RP) can be defined as a group of techniques used to quickly fabricate a scale model of a part or assembly using 3D computer aided design (CAD) data. The concept of RP was developed in the early 1980s in order to provide quicker, cheaper prototypes.

The new RP technologies currently available are Selective Laser Sintering (SLS), Laminated Object Manufacturing (LOM), Fused Deposition modeling (FDM)-viii, Multi-jet printing (MJP)-ix, and 3D printing. Each technology has its own advantages and disadvantages, and are each used for unique applications. A brief overview of the different types of RP is available in Appendix A: An Overview of Rapid Prototyping Processes. With the help of CAD software, a 3D model is created and converted into an STL file, which is currently the standard format in the RP industry. STL files provide a 'triangular representation of the 3D surface geometry' in the form of text-x.

C. Physiology

The human hand consists of five different sets of bones. The carpal bones consists of the greater multangular (GM), navicular (N), lunate (L), triquetrum (T), pisiform (P), lesser multangular (LM), capitated (C), and hamate (H) bones. The metacarpal bones consist of the M-I, II, III, IV, and V bones. The first phalangeal (FP) bones consist of FP-I, II, III, IV, V. The second phalangeal series consists of SP-II, III, IV, and V. The third phalangeal series consists of TP-I, II, III, IV, V.

The different joints in the hand consist of the radio carpal (RC), intercarpal (IC), carpometacarpal (CM), metatarsophalangeal (MP), proximal interphalangeal (PIP), distal interphalangeal (DIP) xvi. Figure 1.1 below indicates the bones located within the human hands with the bones and joints abbreviated as discussed in this section.

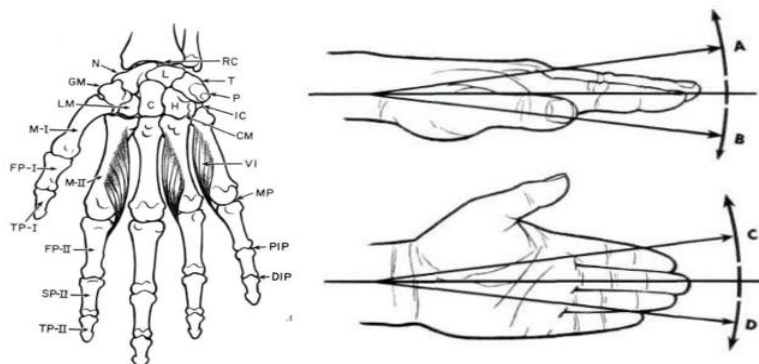


Fig: 1.1 Bones in the Hand and Types of Wrist Movements

Fig: 1.1 indicates the angles of rotation about the wrist. Dorsiflexion or extension is indicated by angle A, flexion or volar flexion is indicated by angle B, radial flexion is indicated by angle C, and ulnar flexion is indicated by angle D.

Table: 1.1 Wrist Flexion Angles

ANGULAR EXTENT OF WRIST FLEXIONS						
Articulation	Dorsal Flexin (deg.)	Volar Flexin (deg.)	Total (deg.)	Ulnar Flexin (deg.)	Radial Flexin(deg.)	Total (deg.)
Capitate-radius	78	44	122	28	17	45
Capitate-lunate	34	22	56	15b	8b	23b
Lunate-radius	44	22	66	13c	9c	22c

II. EXPERIMENTAL DETAILS

A. Components of A 3D Prosthetic Hand

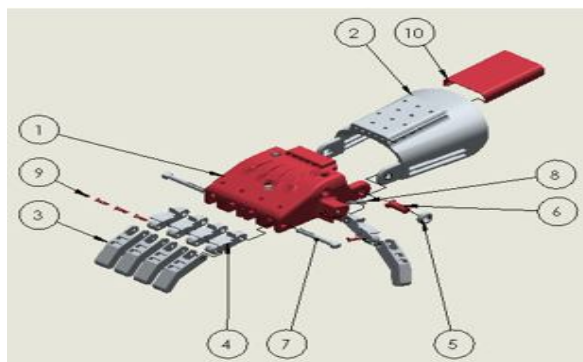


Fig: 2.1 Prototype (Two-Segment Finger) Exploded View

Table: 2.1 Bill of Materials of Prototype Hand Assembly (Two-Segment Finger)

ITEM NO.	DESCRIPTION	QTY.
1	Hand base	1
2	Gauntlet	1
3	Distal Finger	5
4	Proximal Finger	5
5	wrist pin cap	2
6	wrist pin long	2
7	Knuckle Pin	2
8	Thumb To Hand Pin	1
9	Distal to Proximal Pin	5
10	Gauntlet_cover	1

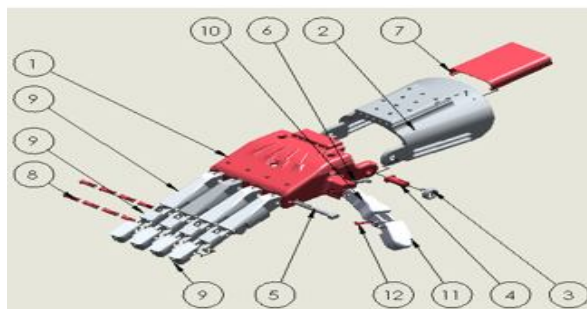


Fig: 2.2 Prortype (Three-Segment Finger)Exploded View

Table: 2.2 Bill of Materials of Prototype Hand Assembly (Three-Segment Finger)

ITEM NO.	DESCRIPTION	QTY.
1	Hand Base	1
2	Gauntlet	1
3	wrist pin cap	2
4	wrist pin long	2
5	knuckle pin	2
6	Thumb To HandPin	1
7	Gauntlet_cover	1
8	Finger pin	8
9	Distal Finger	4
10	Middle Finger	4
11	Proximal Finger	4
12	Proximal Thumb	1
13	Distal Thumb	1
14	Thumb Pin	1

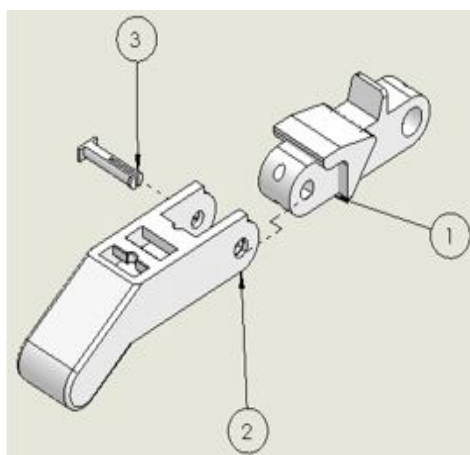


Fig: 2.3 Two-Segment Finger Exploded View

Table: 2.3 Bill of Materials of Two-Segment Finger

ITEM NO.	DESCRIPTION	QTY.
1	Proximal Finger	1
2	Distal Finger	1
3	Finger Pin	1

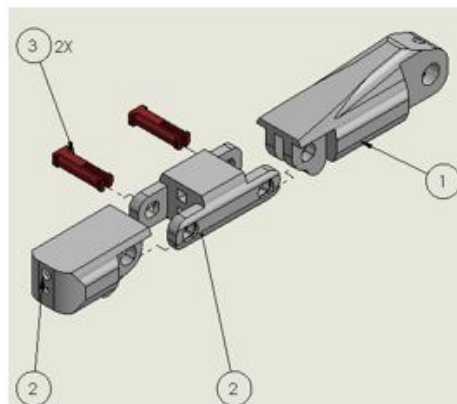


Fig: 2.4 Three-Segment Finger Exploded View

Table: 2.4 Bill of Materials of Three-Segment Finger

ITEM NO.	DESCRIPTION	QTY.
1	Proximal Finger	1
2	Middle Finger	1
3	Distal Finger	1
4	Finger Pin	2

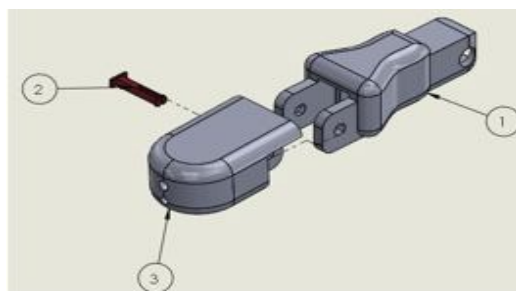


Fig: 2.5 Thumb Exploded View

Table: 2.5 Bill of Materials of Thumb Assembly

ITEM NO.	DESCRIPTION	QTY.
1	Proximal Thumb	1
2	Thumb Pin	1
3	Distal Thumb	1

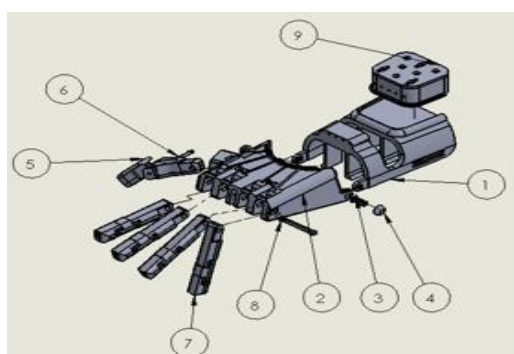


Fig: 2.6 First Generation Hand Exploded View

Table: 2.6 Bill of Materials of First Generation Hand Assembly

ITEM NO.	DESCRIPTION	QTY.
1	Gauntlet	1
2	Hand Base	1
3	Wrist Pin	2
4	Hinge Cap	2
5	Thumb	1
6	Thumb Pin Connection	1
7	Finger	4
8	snap pin for hand	1
9	Gauntlet Tension Mechanism	1

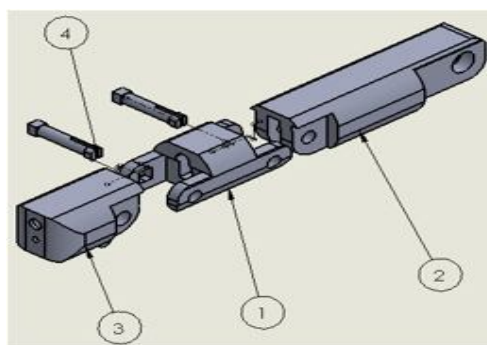


Fig: 2.7 First Generation Finger Exploded View

Table: 2.7 Bill of Materials of First Generation Finger Assembly

ITEM NO.	DESCRIPTION	QTY.
1	Middle Phalange	1
2	Proximal Phalange	1
3	Distal Phalange	1
4	Thumb Pin Connection	2

III. RESULT AND DISCUSSION

A. Kinematic Analysis

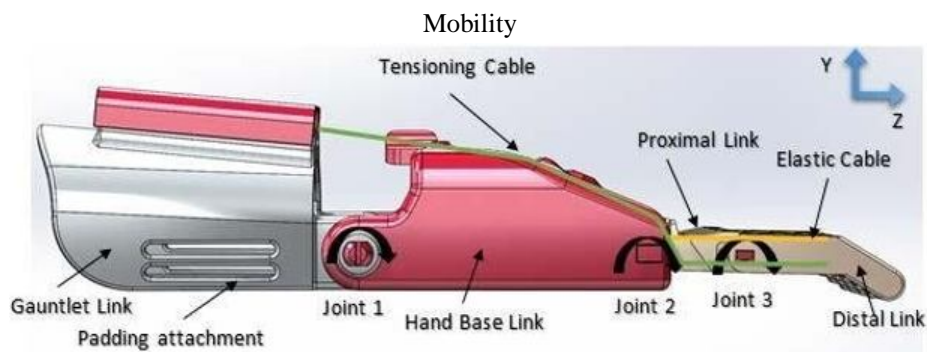


Fig: 3.1 Mobility of Two-Segment Finger-Hand Design

As all 5 fingers functions the same approach, all the fingers will be lumped into one sub-finger in this calculation. Moreover gauntlet is assumed to be grounded because padding attachment to a human's arm. This design provides 3 degree of freedoms. Those degrees of freedoms are independent on its axis. The formula below illustrates the degree of freedom of Figure 3.1.

Number of links (n) = 6, Number of Joints (j) = 6, Degree of Freedom of each pin joint (f) = 1

$$M=3 (n-1)-2j$$

$$M=3 (6-1) - 2(6)$$

$$M=3$$

Where M = mobility, n = number of links, j = number of joints with DOF

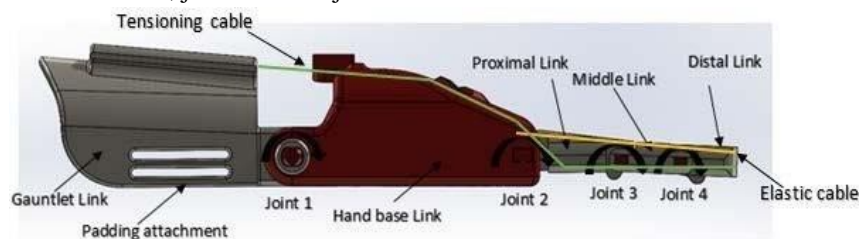


Fig: 3.2 Mobility of Three-Segment Finger-Hand Design

All 5 fingers are lumped onto one finger as it is assumed, they function the same way. Moreover by means of gauntlet is fixed with padding attachment to a human's arm, it is counted as a ground link. For this design, we will have 7 joints and 7 links including the ground. The following formula illustrates the degree of freedom of Figure 3.2.

Number of links (n) = 7 Number of Joints

$$(j) = 7$$

Degree of Freedom of each pin joint

$$(f) = 1 \text{ Kutzbach equation}$$

$$M=3 (n-1)-2j$$

$$M=3 (7-1) - 2(7)$$

$$M=4$$

Where M = mobility, n = number of links, j = number of joints with DOF

B. Design Analysis

In addition to design changes for improved cosmetics, printability, and use of equations, design changes for improved strength were necessary for a functional prosthetic hand. The parts used are all plastic, so withstanding large forces is not to be expected; however, everyday loads should not cause significant stress or deformation to the parts. One way to objectively look at the impact of design changes is to use force analysis through the use of simulations. Finite element analysis (FEA) was performed on several parts to look for excessive forces and deformations. While untested, there was concern that the previous pin hole design was too weak. Analysis was performed and, as predicted, there was significant deformation, as shown in Figure 3.3. The design was revised, and analysis, shown in Figure 3.3 was performed again with significantly less deformation. While the level of deformation is still not ideal, this test was performed with the maximum load being on only one end.



Fig: 3.3 Old Pin Design and New Pin Design

To fit the new pin design, the middle joint needed to be modified to hold the new ends. In addition, because the new pin was larger, the hole size needed to be increased. However, the rounded corners and uniform hole shape distributed the forces more evenly than the smaller holes, which results in less deformation. The changes in hole shape and size, and their resulting deformations are shown in Figure 3.4.

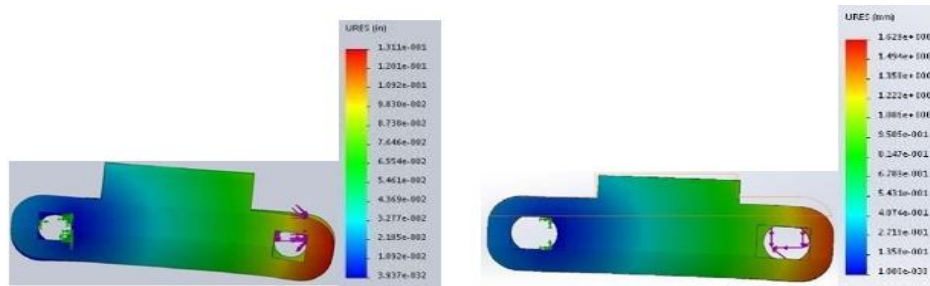


Fig: 3.4 Resulting Deformations

Despite the limitation of the analysis, the simulation run in detail could give reasonable results, which could give insightful information regarding the design conditions. As most of the parts in this product model have complex shapes, the use of curvature mesh instead of standard ones could produce more accurate results. The analysis was performed on depict of forces acting on gauntlet. With the assumption of the weight of an object (which is around 15lb) carried by the hand is vertically downward as shown in Figure 3.5, the reaction forces on gauntlet are vertical along y-axis in the opposite direction.

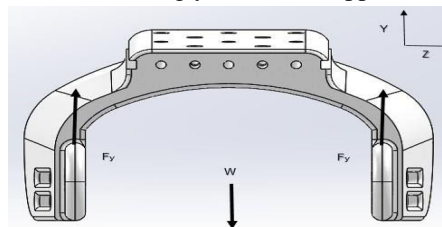


Fig: 3.5 Free Body Diagram of Gauntlet

$$FFFF = WW * 2 = 15 \text{ lbf} * 2 = 7.5 \text{ lbf}$$

*The reaction force, F_y , will be on each side of gauntlet.

Before the analysis, there were also concerns whether the wrist pin of gauntlet would be able to withstand the shear stress and deformation because the reaction forces at the joint, resulting from the applied load, produced shear stresses at the pin on its cross section so it was important to determine the amount of maximum shear stress at the pin. The analysis was performed by fixing the pin at the side surface and applying linear axial load by applying 7.5lbf which is the maximum load.

Most of the 3D printed parts are significantly stronger along the plane of printing than normal to the plane of printing. The pins could resist more shear stress if they were printed along the normal plane than printed vertically which is normal to plane of printing. As the size of pins was revised, the gauntlet wrist joints acquired updates on wrist joints in order to fit the updated wrist pins. By increasing the size of pinhole and wrist joint, the forces acting vertically on joint would be more evenly distributed as potentially reduce the deformation. As shown in Figure 3.5, the vertical forces were applied while top surface is fixed as the gauntlet would be attached to the arm. The maximum displacements due to the loads on the wrist were significantly reduced.

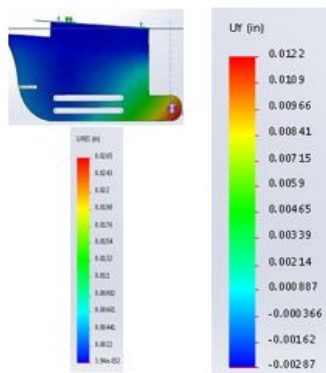


Fig: 3.6 Old Wrist Joint (left) and Updated Wrist Joint (right) of a Gauntlet

In general for 3D printed products, compression loads are not effective for products that are bulky. However for a prosthetic gauntlet, its geometry and material could influence the strength of a product. To find out whether the load from the sides have an adverse effect on the strength of the product in its current shape, the model was simulated again with the fixed top flat part and the two external axial forces applied from the sides as shown in Figure 3.7

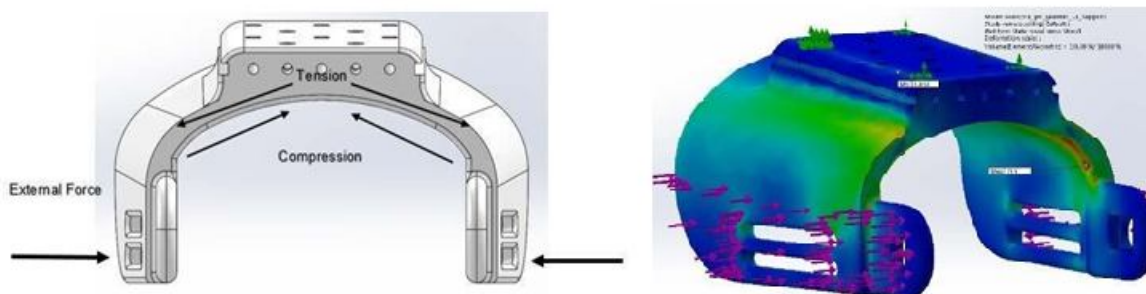


Fig: 3.7 Free Body Diagram of a Gauntlet

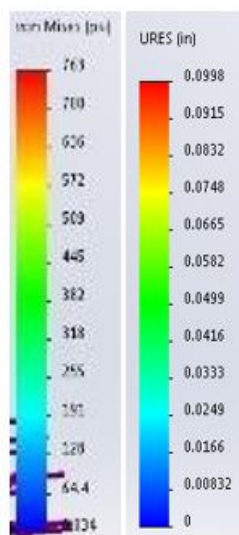
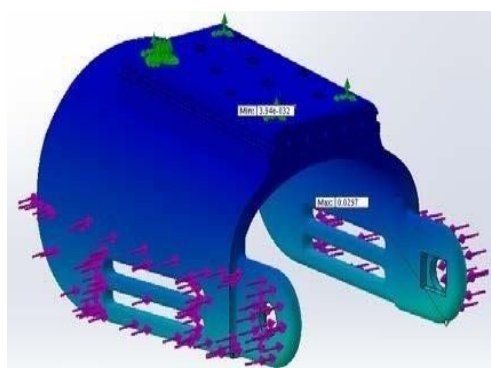


Fig: 3.8 Gauntlet Von Mises Analysis (left) & Deformation Analysis (right)

Figure 3.8 shows that the highest stress area was around the corner and the maximum deformation occurred at the bottom part of gauntlet. This shows the potential failure location of the design where breaking or cracking might occur. Due to the two external axial buckling loads, the product experienced compressive stresses on its interior side and tensile stresses on its exterior side. The products would fail if the external load produced the stress more than yield strength or critical buckling stress, whichever was lower. To avoid this kind of failures, the thickness of the wall and curvature can be increased, as these could reduce the stresses caused by the axial loads and prevent the product from snapping and cracking at the edges where the stresses were concentrated.

C. Parts of Hand Bone

- 1) Hand base
- 2) Proximal finger
- 3) Distal finger
- 4) Gauntlet
- 5) Human bone standardvalue
- a) PH value=7.35-7.45
- b) Salt value=0.4% of body
- c) TDS value =180to280 ppm

(Duromter) for checking hardness of polymer material- (ASTEM) Standard (22.40)polymer (American standard testing & methods) – ASTM- (D Scale) for soft material.

Table: 3.1 hardness value of 3D printing hand bones

PART NAME	T1	T2	T3	(HARDNESS VALUE) “D” SCALE
Hand base	55	60	52	55.66
Proximal finger	48	53	50	50.33
Distal finger	60	55	58	57.66
Gauntlet	65	65	60	63.33

Table: 3.2 Comparison hard value of human bone & 3D printer bone

HUMAN BONE			ARTIFICIAL BONE		
TENSILE	COMPRESSIVE	SHEAR	TENSILE	COMPRESSIVE	SHEAR
150Mpa	250Mpa	450Mpa	126Mpa	250Mpa	200Mpa

Table: 3.3 Comparison between water analyzer best of human bone /3D printing bone

	HUMAN BONE	3D PRINTER BONE	REMARK
PH value	7.35-7.45	7.39	Moderate
Salt value	180 ppm	150 ppm	Best
TDS value	180 to 280 ppm	278 ppm	Best

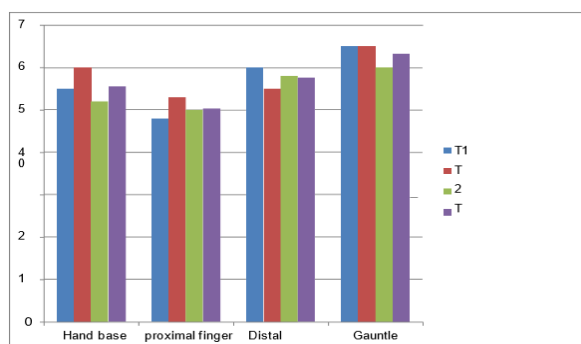


Fig: 3.9 Hardness value of 3D printing hand bone and human bone

IV. CONCLUSION

The artificial human hand parts are fabricated successfully using 3D printing Technology. The various processes are scanning, stereo lithographic, digital file and 3d printing has been practiced. The artificial human parts are made by PLA material and physical, Mechanical and Chemical properties are studied and compared with human bone. Tensile strength, compressive strength, shear strength and bending strength are analyzed byANSYS. The hardness value is physically measured by DURO Meter in ASTM standard. The various chemical test such as salt, pH and TDS have been conducted by water analyzerand compared with human bone. In 2025, artificial bone will play an important role and all hospital is to be provided and print the all parts of human.

REFERENCES

- [1] Widmer MS, Mikos AG. In *Frontiers in Tissue Engineering*, Patrick Jr CW, Mikos AG, McIntire LV, Eds., Elsevier, New York, 1998. Search in Google Scholar
- [2] Hutmacher DW. *Biomaterials* 2000, 21, 2529–2543. Search in Google Scholar
- [3] Esposito Corcione C, Greco A, Maffezzoli A. J. *Therm. Anal. Calorim.* 2003, 72, 687– 693.10.1023/A:1024558506949 Search in Google Scholar
- [4] Esposito Corcione C, Greco A, Maffezzoli A. J. *Appl. Polym. Sci.* 2004, 92, 3484– 3491.10.1002/app.20347 Search in Google Scholar
- [5] Licciulli A, Esposito Corcione C, Greco A, Amicarelli V, Maffezzoli A. J. *Eur. Ceramic Soc.* 2004, 24, 3769–3777.10.1016/j.jeurceramsoc.2003.12.024 Search in Google Scholar
- [6] Licciulli A, Esposito Corcione C, Greco A, Amicarelli V, Maffezzoli A. J. *Eur. Ceramic Soc.* 2005, 25, 1581–1589.10.1016/j.jeurceramsoc.2003.12.003 Search in Google Scholar
- [7] Esposito Corcione C, Greco A, Licciulli A, Maffezzoli A. J. *Mater. Sci.* 2005, 40, 1– 6.10.1007/s10853-005-5682-5 Search in Google Scholar
- [8] Esposito Corcione C, Montagna F, Greco A, Licciulli A, Maffezzoli A. *Rapid Prototyp.J.* 2006, 12, 184–188.10.1108/13552540610682688 Search in Google Scholar
- [9] Esposito Corcione C, Greco A, Maffezzoli A. *Polym. Eng. Sci.* 2006, 46, 493– 502.10.1002/pen.20488 Search in Google Scholar
- [10] Scalera F, Esposito Corcione C, Montagna F, Sannino A, Maffezzoli A. *Ceram. Int.* 2014, 40, 15455–15462.10.1016/j.ceramint.2014.06.117 Search in Google Scholar
- [11] Esposito Corcione C. J. *Polym. Eng.* 2014, 34, 85–93. Search in Google Scholar
- [12] Esposito Corcione C, Striani R, Montagna F, Cannoletta D. *Polym. Advan. Technol.* 2015, 26, 92– 98.10.1002/pat.3425 Search in Google Scholar.
- [13] Birtchnell T, Urry J. *Futures* 2013, 50, 25–34.10.1016/j.futures.2013.03.005 Search in Google Scholar.
- [14] Rezwan K, Chen QZ, Blaker JJ, Boccaccini AR. *Biomaterials* 2006, 27, 3413-1.10.1016/j.biomaterials.2006.01.039 Search in Google Scholar
- [15] Navarro M, Aparicio C, Charles-Harris M, Ginebra MP, Engel E, Planell JA. *Adv. Polym. Sci.* 2006, 200, 209–231.10.1007/12_068 Search in Google Scholar.



10.22214/IJRASET



45.98



IMPACT FACTOR:
7.129



IMPACT FACTOR:
7.429



INTERNATIONAL JOURNAL FOR RESEARCH

IN APPLIED SCIENCE & ENGINEERING TECHNOLOGY

Call : 08813907089  (24*7 Support on Whatsapp)